

Analysis of multiparticle production using split-bin correlation functions

David Seibert*

School of Physics and Astronomy, University of Minnesota, Minneapolis, Minnesota 55455

Sergei Voloshin[†]

Theoretical Physics Institute, University of Minnesota, Minneapolis, Minnesota 55455

(Received 3 May 1990)

We discuss the study of correlations in multiparticle processes, using split-bin correlation functions (SBCF's). We show how SBCF's can be used to study different production mechanisms, such as production via jetlike or resonancelike sources. We illustrate some possibilities with calculations of various SBCF's in simple models. One of the main advantages of SBCF's is the possibility of using transverse-energy correlations as well as multiplicity correlations in order to differentiate the various mechanisms of particle production. We show that in general the transverse-energy SBCF's and the multiplicity SBCF's are very similar, but also discuss some models for which these classes of SBCF's will be different. Finally, we provide useful formulas for the analysis of SBCF data using simple analytic models, including effects due to curvature of the single-particle distribution.

I. INTRODUCTION

We have proposed¹ the use of split-bin correlation functions (SBCF's) in order to facilitate the study of short-range correlations in multiparticle production processes. Scaled-factorial-moment analysis^{2,3} shows that the correlations seen in heavy-ion collisions are much larger than those seen in leptonic and hadronic collisions, when corrected for multiplicity effects.^{3,4} There is also evidence from \bar{p} - p data^{5,4} for structure in hadronic correlations on the scale of 0.1 units of rapidity. These large correlations and small-scale structure are not yet understood. We suggest that the use of SBCF's could lead to greater understanding of the structure and origin of hadronic correlations than is possible with currently used correlation functions.

Measurement of the differences between various SBCF's provides much clearer information about the sources of correlations than measurements of standard two-particle correlation functions alone. The very clear physical meanings of the various SBCF's facilitate the construction of SBCF's to differentiate between specific models of hadronic correlations. The flexibility of SBCF's makes discussion of the full possibilities of this approach impossible, so we will show only the most simple and remarkable advantages of this technique.

We begin by defining the general form for split-bin correlation functions in Sec. II. We define S_2 , the simplest SBCF, and compare it to the second scaled factorial moment F_2 . We then discuss various uses for SBCF's. In Sec. III, we first calculate the effect on S_2 of curved single-particle distributions. We then calculate S_2 as a function of the total multiplicity N , the number of correlated pairs N_c , and the distribution of rapidity separations for correlated pairs $p_c(|y_2 - y_1|)$. Finally, we derive multiplicity scaling relations that can be used to compare SBCF data for different event samples.

In Sec. IV, we use simple models to illustrate the potential value of SBCF's for distinguishing effects of different multiparticle production mechanisms. We show that S_2 is likely to be larger than S_2^ϕ for "resonancelike" production mechanisms, while the converse is true for "jetlike" production mechanisms. We show that measurements of transverse-energy SBCF's can be used to differentiate models, just as we can use measurements of multiplicity SBCF's. We also show that it is possible for transverse-energy and multiplicity SBCF's to give different results, yielding further constraints on models of hadronization. We then show a novel approach, using SBCF's, to the study of azimuthal angle correlations. Finally, we discuss ways to use SBCF's to selectively study the roles of the various resonances, jets, Bose-Einstein correlations, and other effects thought to be significant in multiparticle production.

II. SPLIT-BIN CORRELATION FUNCTIONS

The general form of the split-bin correlation function of order i is

$$S_i(M) = M^{i-1} \frac{\sum_{m=1}^M \left\langle \prod_{j=1}^i n_{m,j} \right\rangle}{\left\langle \prod_{j=1}^i N_j \right\rangle}, \quad (1)$$

where the rapidity window is divided into M equal bins, each bin is divided into i sub-bins, $n_{m,j}$ is the number of particles in the j th sub-bin of the m th bin, and N_j is the number of particles in the j th sub-bin of the entire rapidity window. In this paper, we concentrate on second-order SBCF's such as

$$S_2(M) = M \frac{\sum_{m=1}^M \langle n_m^L n_m^R \rangle}{\langle N^L N^R \rangle}, \quad (2)$$

where $n_m^{L(R)}$ is the number of particles in the left (right) half of the m th bin, and $N^{L(R)}$ is the number of particles in the left (right) half of the rapidity window.

We could also, in analogy to the inclusive scaled factorial moments,⁶ construct the second-order SBCF

$$\tilde{S}_2(M) = 4M \frac{\sum_{m=1}^M \langle n_m^L n_m^R \rangle}{\langle N \rangle^2}, \quad (3)$$

where N is the total number of particles in the rapidity window. However, \tilde{S}_2 exhibits fictitious long-range correlations,⁷ unlike S_2 . Thus, experimenters who construct \tilde{S}_2 must be careful when comparing events with different multiplicities.

S_2 can also be expressed in terms of rapidity densities, yielding

$$S_2(M) = \frac{M \sum_{m=1}^M \int_{y_0}^{y_0+\Delta Y/2} dy_1 \int_{y_0+\Delta Y/2}^{y_0+\Delta Y} dy_2 \rho^{(2)}(y_1, y_2)}{\int_{y_0}^{y_0+\Delta Y/2} dy_1 \int_{y_0+\Delta Y/2}^{y_0+\Delta Y} dy_2 \rho^{(2)}(y_1, y_2)}, \quad (4)$$

where $y_i = y_0 + i\Delta Y/2M$. It is readily apparent from the definition (4) that $S_2(M)$ will exhibit a power-law divergence as $M \rightarrow \infty$ if intermittency occurs, since the mean value of $\rho^{(2)}$ then has a power-law divergence.

We can also construct split-bin correlation functions using transverse energy $\mathcal{E}^T = \mathcal{E} \sin\theta$, where \mathcal{E} is the energy in a bin and θ is the angle with respect to the beam direction, measured from the primary interaction vertex. This construction gives a transverse-energy analogue for every multiplicity correlation function. For example, the transverse-energy analogue of S_2 is

$$S_2^{\mathcal{E}}(M) = M \frac{\sum_{m=1}^M \langle \mathcal{E}_{m,L}^T \mathcal{E}_{m,R}^T \rangle}{\langle E_L^T E_R^T \rangle}, \quad (5)$$

where $\mathcal{E}_{m,L(R)}^T$ is the transverse energy in the left (right) half of the m th bin, and $E_{L(R)}^T$ is the transverse energy in the left (right) half of the rapidity window.

$S_2^{\mathcal{E}}$ is very close to S_2 for many models of multiparticle production, and all of the analytic formulas that we will present for S_2 in Sec. III hold for $S_2^{\mathcal{E}}$ as well if there is only one transverse-energy scale. This is not true for all models; however, such general problems are too difficult to pursue analytically. Instead, we compare S_2 and $S_2^{\mathcal{E}}$ for some of the simple models of Sec. IV, in order to show qualitative features of the behavior of split-bin correlation functions. We also compare some of the other second-order SBCF's with their transverse-energy analogues. We will not present the definitions of the remaining analogues, as each is obtained simply by substituting \mathcal{E}^T for n everywhere in the definition of the SBCF, just as $S_2^{\mathcal{E}}$ is obtained from S_2 .

III. BEHAVIOR OF SBCF's

In this section, we first show how to calculate the effects of curvature in the single-particle distribution. We then show how to calculate S_2 in terms of the total multiplicity N , the number of correlated pairs N_c , and the distribution of rapidity separations for correlated pairs $p_c(|y_1 - y_2|)$. Finally, we show that S_2 should, under reasonable assumptions, obey a multiplicity scaling law that is almost identical to the multiplicity scaling law proposed for scaled factorial moments.³

If the particle distribution dN/dy is flat, and particle rapidities are uncorrelated, the two-particle density $\rho^{(2)}$ is independent of y_1 and y_2 . In this case, it is trivial to show that $S_2(M) = 1$ for all values of M . If rapidities are uncorrelated but dN/dy is not constant, $S_2(M) \neq 1$. In this case, we recommend that experimenters present the value of S_2 due to the curved rapidity distribution alone, S_2^c , along with their data. It is possible to use a multiplicative correction factor for curvature effects, as is suggested for scaled factorial moments,⁸ but it is more difficult to analyze corrected data because the curvatures of the rapidity distributions, and thus the correction factors, may be different for correlated and uncorrelated pairs.

The component of S_2 due to curvature of the single-particle distribution (for uncorrelated particles), S_2^c , is

$$S_2^c(M) = M \frac{\sum_{m=1}^M \langle n_m^L \rangle \langle n_m^R \rangle}{\langle N^L \rangle \langle N^R \rangle}. \quad (6)$$

S_2^c can also be expressed in terms of the normalized rapidity distributions

$$p_N(y) = \rho_N(y) / N, \quad (7)$$

where N is the multiplicity and $\rho_N(y)$ is the single-particle rapidity density for events with multiplicity N . We consider here just the simplest case where

$$p_N(y) = p(y), \quad (8)$$

independent of N . In this case, the two-particle density is

$$\rho^{(2)}(y_1, y_2) = \langle N(N-1) \rangle p(y_1) p(y_2), \quad (9)$$

where $\langle N(N-1) \rangle$ is the mean number of pairs of particles produced.

We first calculate the denominator of S_2^c :

$$\begin{aligned} & \int_{y_0}^{y_0+\Delta Y/2} dy_1 \int_{y_0+\Delta Y/2}^{y_0+\Delta Y} dy_2 \rho^{(2)}(y_1, y_2) \\ &= \langle N(N-1) \rangle \int_{y_0}^{y_0+\Delta Y/2} dy_1 p(y_1) \int_{y_0+\Delta Y/2}^{y_0+\Delta Y} dy_2 p(y_2). \end{aligned} \quad (10)$$

If the window is picked so that $p(y)$ is symmetric, which is the usual case, we have

$$\int_{y_0}^{y_0+\Delta Y/2} dy p(y) = \int_{y_0+\Delta Y/2}^{y_0+\Delta Y} dy p(y) = \frac{1}{2}. \quad (11)$$

Inserting the values of the integrals from Eq. (11) in Eq. (10), we obtain

$$\int_{y_0}^{y_0+\Delta Y/2} dy_1 \int_{y_0+\Delta Y/2}^{y_0+\Delta Y} dy_2 \rho^{(2)}(y_1, y_2) = \frac{1}{4} \langle N(N-1) \rangle. \quad (12)$$

The numerator of S_2^c is also fairly simple:

$$\begin{aligned} M \sum_{m=1}^M \int_{y_{2m-2}}^{y_{2m-1}} dy_1 \int_{y_{2m-1}}^{y_{2m}} dy_2 \rho^{(2)} \\ = M \sum_{m=1}^M \langle N(N-1) \rangle \\ \times \int_{y_{2m-2}}^{y_{2m-1}} dy_1 p(y_1) \int_{y_{2m-1}}^{y_{2m}} dy_2 p(y_2). \end{aligned} \quad (13)$$

This leads to a simple expression:

$$S_2^c(M) = 4M \sum_{m=1}^M \int_{y_{2m-2}}^{y_{2m-1}} dy_1 p(y_1) \int_{y_{2m-1}}^{y_{2m}} dy_2 p(y_2). \quad (14)$$

The most accurate determination of S_2^c is made by direct computation from dN/dy data, using Eq. (6). There is no general closed-form expression for the sum of integrals in Eq. (14), but it can be approximated well by an expansion in powers of $1/M$ when M is large. Large M corresponds to small bin sizes, and the limit of zero bin size is the most interesting case for the study of intermittency, so we next calculate S_2^c in the limit $M \rightarrow \infty$.

We first approximate the integrals over the m th subbins by expanding $p(y)$ to lowest order in $\delta y = \Delta Y/M$, obtaining

$$S_2^c(M) = M \sum_{m=1}^M \delta y^2 [p^2(y_{2m-1}) + O(\delta y^2)]. \quad (15)$$

After converting the sum to an integral, we obtain

$$S_2^c(\delta y) = \Delta Y \int_{y_0}^{y_0+\Delta Y} dy p^2(y) + O(\delta y^2). \quad (16)$$

We can also express S_2^c as a function of the fractional deviation of p from its mean value ($\bar{p} = 1/\Delta Y$), $q = p\Delta Y - 1$:

$$S_2^c(\delta y) = 1 + \left[\frac{1}{\Delta Y} \int_{y_0}^{y_0+\Delta Y} dy q^2 \right] + O(\delta y^2). \quad (17)$$

It is obvious that S_2^c can be written in the form

$$S_2^c(\delta y) = 1 + \delta s_2^c(\delta y), \quad (18)$$

where the correction due to curvature is

$$\delta s_2^c(0) = \frac{1}{\Delta Y} \int_{y_0}^{y_0+\Delta Y} dy q^2 = \overline{q^2}. \quad (19)$$

Equation (19) is very useful for estimating the maximum correction due to curvature for a given window ΔY . We can see directly from this equation that, independent of the function p , if we pick ΔY so that p is never less than 90% of its peak value, the maximum possible value of δs_2^c is 0.01.

We can calculate $S_2(M)$ for a simple system with N_c correlated pairs of particles and a total of N particles (with a flat rapidity distribution) if we know the distribution of rapidity separations for the correlated pairs,

$p_c(|y_1 - y_2|)$. We define N_c so that a source of n_p inter-correlated particles produces $n_p(n_p - 1)$ correlated pairs. For example, an event that contains a single resonance that decays into six particles would have $N_c = 30$, while an event that contains two resonances, that decay into three particles each, would have $N_c = 12$.

We have in total $N(N-1)$ pairs of particles, so we must have $N(N-1) - N_c$ uncorrelated pairs. We begin by splitting the two-particle rapidity density into two parts:

$$\rho^{(2)} = \rho_u^{(2)} + \rho_c^{(2)}, \quad (20)$$

where $\rho_u^{(2)}$ comes from the uncorrelated pairs and $\rho_c^{(2)}$ comes from the correlated pairs. The uncorrelated two-particle density is simply

$$\rho_u^{(2)} = \frac{N(N-1) - N_c}{\Delta Y^2}, \quad (21)$$

and we obtain

$$\begin{aligned} M \sum_{m=1}^M \int_{y_{2m-2}}^{y_{2m-1}} dy_1 \int_{y_{2m-1}}^{y_{2m}} dy_2 \rho_u^{(2)}(y_1, y_2) \\ = \int_{y_0}^{y_0+\Delta Y/2} dy_1 \int_{y_0+\Delta Y/2}^{y_0+\Delta Y} dy_2 \rho_u^{(2)}(y_1, y_2) \\ = \frac{N(N-1) - N_c}{4}. \end{aligned} \quad (22)$$

If we assume that the distribution of the centers of momentum of the correlated pairs is flat, the correlated two-particle density is

$$\rho_c^{(2)}(y_1, y_2) = \frac{N_c}{\Delta Y} p_c(|y_1 - y_2|). \quad (23)$$

We then obtain

$$M \sum_{m=1}^M \int_{y_{2m-2}}^{y_{2m-1}} dy_1 \int_{y_{2m-1}}^{y_{2m}} dy_2 \rho_c^{(2)}(y_1, y_2) = N_c \Delta Y g(\delta y) \quad (24)$$

and

$$\int_{y_0}^{y_0+\Delta Y/2} dy_1 \int_{y_0+\Delta Y/2}^{y_0+\Delta Y} dy_2 \rho_c^{(2)}(y_1, y_2) = N_c \Delta Y g(\Delta Y), \quad (25)$$

where

$$g(z) = \frac{1}{z^2} \left[\int_0^{z/2} dy y p_c(y) + \int_{z/2}^z dy (z-y) p_c(y) \right]. \quad (26)$$

Combining Eqs. (22), (24), and (25), we find

$$S_2(\delta y) = \frac{[N(N-1) - N_c] + 4N_c \Delta Y g(\delta y)}{[N(N-1) - N_c] + 4N_c \Delta Y g(\Delta Y)}. \quad (27)$$

Equation (27) is most interesting in the limit $N_c \ll N(N-1)$, which is valid in almost any possible model for ultrarelativistic collisions. In this case, we further simplify Eq. (27):

$$S_2(\delta y) = 1 + \frac{4N_c \Delta Y}{N(N-1)} \left[g(\delta y) - g(\Delta Y) + O \left[\frac{N_c}{N(N-1)} \right] \right]. \quad (28)$$

Equation (28) leads to multiplicity scaling for S_2 that is identical to the multiplicity scaling for scaled factorial moments.

If the various sources of correlated particles do not interact, N_c is proportional to the number of sources, which is most likely proportional to the multiplicity N . We can then write

$$N_c = n_c \frac{fN}{n_p}, \quad (29)$$

where n_p is the number of particles produced per source, f is the fraction of produced particles that come from sources, and n_c is the number of correlated pairs produced per source. Substituting N_c from Eq. (29) in Eq.(28), we obtain

$$S_2(\delta y) = 1 + 4\Delta Y f \frac{n_c}{Nn_p} \left[g(\delta y) - g(\Delta Y) + O \left[\frac{1}{N} \right] \right]. \quad (30)$$

For the flat distributions that we are considering, $dN/dy = N/\Delta Y$, and we find

$$[S_2(\delta y) - 1](dN/dy) = 4f \frac{n_c}{n_p} [g(\delta y) - g(\Delta Y)] + O \left[\frac{1}{N} \right]. \quad (31)$$

The scaling law (32) can be used to compare values of S_2 for different event samples which are believed to be produced by similar processes. Because f , n_c , and n_p are independent of δy , it follows immediately from the scaling law (31) that the *shape* of $S_2 - 1$ depends only on the function g . Thus, if correlated pairs are produced with the same distribution of rapidity separations in two different event samples, the shape of $S_2 - 1$ will be the same for the two samples, *independent* of the relative numbers of correlated pairs in the samples. For example, if we consider event samples a and b , such that the distribution of rapidity separations for correlated pairs is the same for the two samples, we will find that

$$\frac{(dN/dy)_a [S_2(\delta y) - 1]_a}{(dN/dy)_b [S_2(\delta y) - 1]_b} = \frac{f_a (n_c/n_p)_a}{f_b (n_c/n_p)_b} = \text{const}, \quad (32)$$

independent of δy .

If we have two different event samples where the shape of $S_2 - 1$ is approximately the same, we can then assume that the function g is the same for the two samples. In this case, we can use the multiplicity scaling law (32) to compare the relative source sizes (for correlated pairs) in the two samples. For instance, if we assume that f is the same for samples a and b , we find

$$\left[\frac{n_c}{n_p} \right]_a = \frac{[S_2(\delta y) - 1]_a (dN/dy)_a}{[S_2(\delta y) - 1]_b (dN/dy)_b} \left[\frac{n_c}{n_p} \right]_b. \quad (33)$$

If we furthermore assume that all of the particles from a given source are intercorrelated, $n_c/n_p = n_p - 1 \approx n_p$, and we find that

$$(n_p)_a = \frac{[S_2(\delta y) - 1]_a (dN/dy)_a}{[S_2(\delta y) - 1]_b (dN/dy)_b} (n_p)_b. \quad (34)$$

Thus, if we know the source sizes for event sample b , we can determine the source sizes for related event sample a by measuring S_2 .

We postpone the definition of further SBCF's until the next section, in which we discuss ways that SBCF data can be used to test various classes of models. We will not calculate the corrections due to curvature for any other SBCF, as this calculation is essentially identical to that given for S_2 . We also will not discuss scaling for any other SBCF's, as they all obey the scaling law (32) and its corollaries (33) and (34) if Eq. (29) is valid. Equations (30) and (31) will be somewhat modified, as the function g will not be the same for all SBCF's, but the essential character of these equations remains the same for any SBCF.

IV. USING SBCF'S TO TEST CLASSES OF MODELS

SBCF's are very convenient tools for checking different assumptions of hadron production mechanisms. Because the physical content of SBCF's is very clear, it is possible to construct specific SBCF's to test various properties.

It is difficult to calculate all of these SBCF's from analytic models, so we compare the various SBCF's using Monte Carlo analyses of several simple models. We do not attempt to describe the experimental data, but only to illustrate some possibilities of SBCF's. In our models, all direct particles are produced with random rapidities given by the distribution

$$\frac{dn}{dy} = D \left[1 - \exp \left[\frac{y - y_{\max}}{2} \right] \right] \left[1 - \exp \left[\frac{y_{\max} - y}{2} \right] \right]. \quad (35)$$

Here $y_{\max} = \ln s$ (we take $s = 400 \text{ GeV}^2$), and D is the appropriate normalization factor. The multiplicity is given by a Poisson distribution, with an average of 14 particles in the rapidity window $(-2, 2)$.

All correlations in our models are provided by decays of direct particles. We assume that some fraction of the direct particles are unstable and decay into two pions, and that the remainder of the direct particles are pions. These unstable particles are assumed to decay isotropically, resulting in a distribution of rapidity separations for the decay products that is specified by the maximum rapidity separation Δy_{\max} between products, measured in the rest frame of the direct particle.

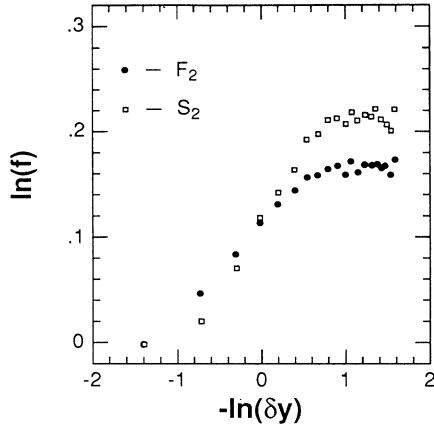


FIG. 1. Comparison of F_2 and S_2 vs δy for the model given in the text.

The parameter Δy_{\max} is related to the masses of the unstable particles and pions, respectively, m_u and m_π , by

$$\Delta y_{\max} = 2 \ln \frac{m_u/2 + \sqrt{(m_u/2)^2 - m_\pi^2}}{m_\pi}. \quad (36)$$

The distribution function for transverse momenta of

direct particles (both stable and unstable hadrons) is taken to be

$$P(p_T) \sim p_T \exp(-p_T^2/2\bar{p}^2). \quad (37)$$

Unless otherwise stated, we used $\bar{p} = 0.3$ GeV, corresponding to $\langle p_T \rangle \approx 0.36$ GeV, and assume that 75% of the direct particles are unstable and have $\Delta y_{\max} = 0.4$.

The first feature of SBCF's that we discuss is their insensitivity (in comparison with scaled factorial moments) to pairs of particles with very small rapidity differences. We demonstrate this insensitivity in Fig. 1, where the results of our model for F_2 and S_2 are presented. The linear growth of F_2 for large δy is due to the decrease in the average multiplicity, as correlations on all scales less than δy contribute to F_2 . Because of this initial linear growth, the slope of F_2 is usually largest for large δy .

The behavior of S_2 is quite different. In general, $S_2 - 1 \sim (1/\delta y^2 - 1/\Delta Y^2)$ for $\delta y \approx \Delta Y$, and reaches its maximum slope when δy is approximately equal to the correlation rapidity scale. This behavior of S_2 for large δy is responsible for the insensitivity of S_2 to double counting of tracks, as double counting is equivalent to the production of spurious correlations with a scale of zero units of rapidity.

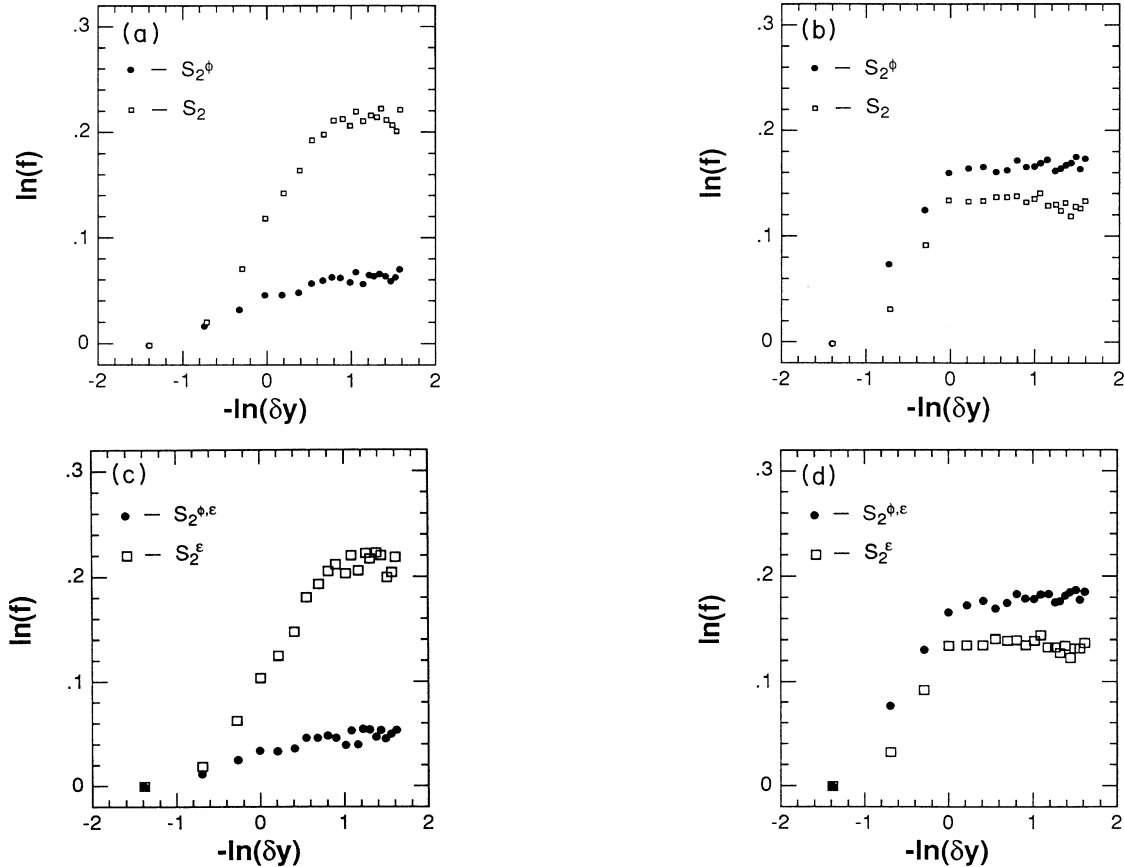


FIG. 2. Comparisons of SBCF's for the models given in the text. (a) S_2 and S_2^ϕ for resonancelike sources. (b) S_2 and S_2^ϕ for jetlike sources. (c) S_2^ϵ and $S_2^{\phi,\epsilon}$ for resonancelike sources. (d) S_2^ϵ and $S_2^{\phi,\epsilon}$ for jetlike sources.

The main feature of jetlike production mechanisms is production of clumps of particles with equal and opposite momenta $p \gg \langle p_T \rangle$ (in the rest frame of the jet). In resonancelike production, particles are produced in an isotropic manner, with momenta $p \sim \langle p_T \rangle$. Thus, we can look for jetlike and resonancelike production mechanisms by testing whether the correlated pairs have similar transverse momenta (for resonances) or opposite transverse momenta (for jets).

The simplest test is to compare the SBCF's S_2 and S_2^ϕ , where S_2^ϕ is constructed by splitting each of the rapidity bins into two equal sub-bins in azimuthal angle ϕ . This production gives

$$S_2^\phi(M) = M \frac{\sum_{m=1}^M \langle n_m^+ n_m^- \rangle}{\langle N^+ N^- \rangle}, \quad (38)$$

where $n_m^{+(-)}$ is the number of particles in the m th bin with $\cos\phi > (<) 0$, and $N^{+(-)}$ is the number of particles in the rapidity window with $\cos\phi > (<) 0$. S_2^ϕ gives the strong signal when rapidities are correlated and azimuthal angles are anticorrelated. If $S_2^\phi > S_2$, the correlations are most likely produced by jetlike mechanisms. Conversely, if $S_2 > S_2^\phi$ the correlations are probably produced by resonancelike mechanisms where the transverse momentum of the resonance is greater than or equal to the momenta of its decay products.

In Fig. 2, we compare S_2 with S_2^ϕ and S_2^ϵ with $S_2^{\phi,\epsilon}$ for our model, where S_2^ϵ and $S_2^{\phi,\epsilon}$ are the \mathcal{E}^T equivalents of S_2 and S_2^ϕ . We use different values of \bar{p} to simulate resonancelike and jetlike production mechanisms. For resonancelike production (a) and (c) we use $\bar{p} = 0.3$ GeV, and for jetlike production (b) and (d) we use $\bar{p} = 0$. As we expect, $S_2 > S_2^\phi$ for (a) and (c), while the converse is true for (b) and (d). It is also apparent from Fig. 2 that multiplicity and transverse-energy correlation functions can be used interchangeably for this type of comparison, and that their values are very similar.

Of course, typical models of production mechanisms are much more complicated than our simple models, but we can still obtain strong constraints on models by comparing SBCF's. One advantage of comparisons is that the effects of the shape of the single-particle distribution are the same for any two second-order SBCF's *in the limit* $\delta y \rightarrow 0$, and so comparison tests can be performed without correcting the data. Thus, comparison tests can be constructed in order to test very specific features of a production mechanism, independent of other features such as the average multiplicity or the shape of the single-particle distribution.

In most models, all particles have approximately the same mean transverse energy, whether they are produced directly or indirectly. As a result, the transverse energy SBCF's are often nearly equal to the multiplicity SBCF's. In Fig. 3, we compare S_2 and S_2^ϵ for two simple models. For the first model, (a), we use our standard parameters, and we find that S_2 and S_2^ϵ are very close. For the second model, (b), we assume that only 10% of the direct particles are unstable, and that these unstable particles have a mass of approximately 3 GeV. In this case, we

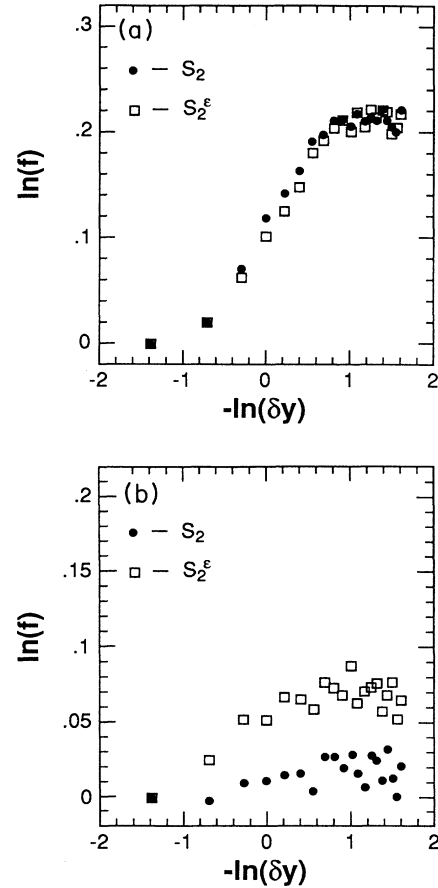


FIG. 3. Comparisons of S_2 and S_2^ϵ . (a) Typical transverse momenta. (b) Large transverse momenta.

find that the shapes of the two SBCF's are the same, but that $S_2^\epsilon \gg S_2$, as the mean transverse energy of the correlated particles is much greater than the mean transverse energy of the uncorrelated direct particles. We can thus use comparisons of multiplicity and transverse-energy SBCF's to constrain models, but this can be difficult as the single-particle rapidity distribution is not always equal to the transverse-energy rapidity distribution, and thus the SBCF's might need correction before they are compared.

The comparison of S_2 and S_2^ϕ is the simplest way to study production mechanisms, but there are many other possibilities, such as studies of SBCF's in ϕ . We can study correlations with different ϕ symmetries by using various SBCF's. For example, we use S_2 to look for correlations in ϕ , and use the new SBCF S_2^{op} , where we take the products of particle numbers in opposite rapidity bins, to look for anticorrelations in ϕ .

We can also selectively study the correlations produced by resonances with different masses, by constructing SBCF's using only particles with $p_T > p_{T,\text{cut}}$. In Fig. 4, we compare \tilde{S}_2 and \tilde{S}_2^{op} as a function of M (the number of ϕ bins), both with and without a transverse-momentum cut, using the single rapidity bin $(-1, 1)$. These SBCF's have

a normalization that is equivalent to the normalization of the inclusive scaled factorial moments, as in Eq. (3).

Figure 4(a) shows results from our simple model with $\Delta y_{\max} = 1.5$, corresponding to the decay of an unstable particle with mass $m_u \approx 0.7$ GeV into two pions, and no p_T cut, while in Fig. 4(c) we use $\Delta y_{\max} = 2.0$ ($m_u \approx 1$ GeV), again with no cut. We use the parameters from (a) and (c) in (b) and (d), respectively, but we now accept only particles with $p_T > 0.3$ GeV. Almost all correlations from the unstable particles with $\Delta y_{\max} = 1.5$ vanish, while the correlations due to the unstable particles with $\Delta y_{\max} = 2.0$ are enhanced.

If we can identify the charges of all particles, we can construct various useful SBCF's. For example, we could construct an SBCF that is "blind" to Bose-Einstein correlations by multiplying the number of negatively charged particles in the left sub-bin by the number of positively charged particles in the right sub-bin. It is possible to attempt to remove Bose-Einstein correlations from scaled-factorial-moment data, but much clearer results can be obtained using SBCF's.

Up to now we have discussed only second-order SBCF's. However, higher-order SBCF's may provide some additional constraints on models that have a great

deal of symmetry. For example, we can search for the presence of disklike sources by using high-order SBCF's, such as

$$S_j(M) = M^{j-1} \frac{\sum_{m=1}^M \left\langle \prod_{i=1}^j n_m^{(i)} \right\rangle}{\left\langle \prod_{i=1}^j N^{(i)} \right\rangle}, \quad (39)$$

where every rapidity bin is divided into j azimuthal angle sub-bins. By observing the dependence of S_j on M and j , we can search for disklike sources, and estimate their spread in rapidity and the number of particles produced from each source.

V. SUMMARY

We have discussed the use of a new family of correlation functions for the study of multiparticle processes, the split-bin correlation functions. These correlation functions are easier to measure than the scaled factorial moments, because they are less susceptible to systematic errors such as double counting of tracks and varying detector efficiencies. Split-bin correlation functions can

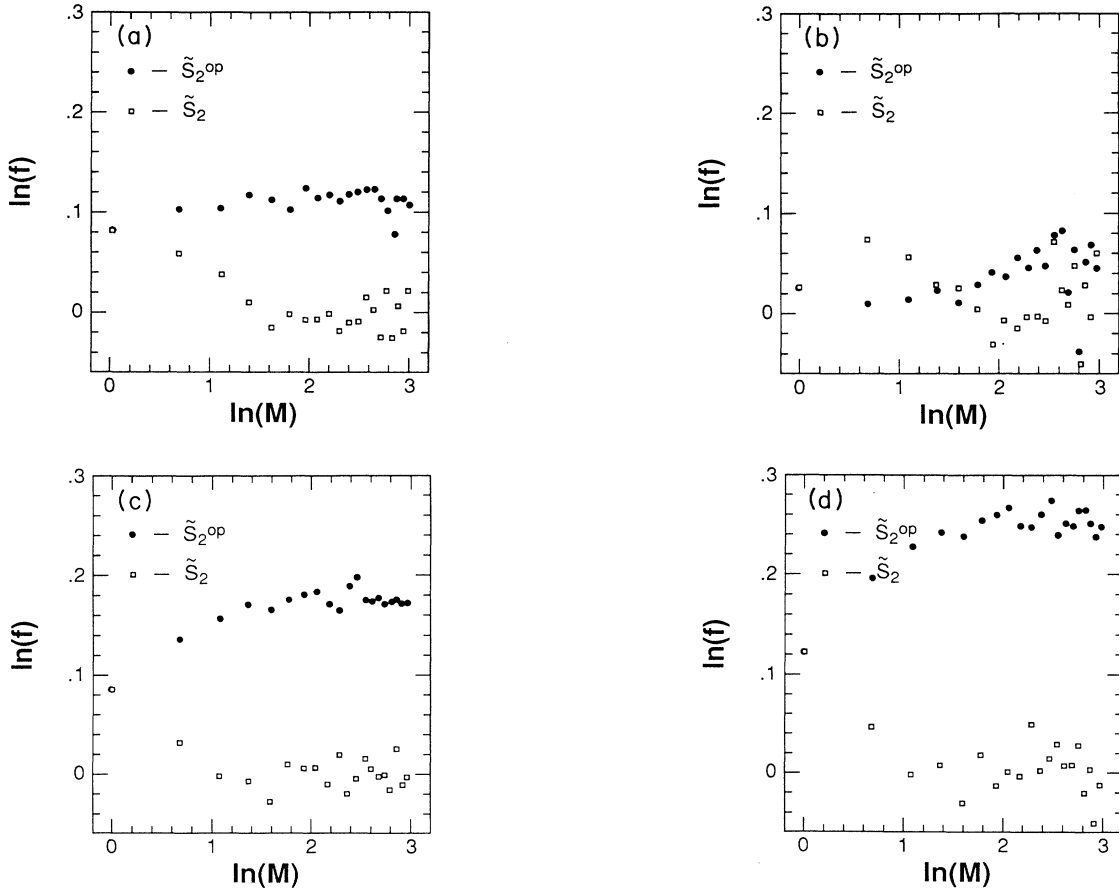


FIG. 4. Comparisons of \tilde{S}_2 and \tilde{S}_2^{op} . (a) $\Delta y_{\max} = 1.5$, all values of p_T . (b) $\Delta y_{\max} = 1.5$, $p_T > 0.3$ GeV. (c) $\Delta y_{\max} = 2.0$, all values of p_T . (d) $\Delta y_{\max} = 2.0$, $p_T > 0.3$ GeV.

also be measured using continuous variables such as \mathcal{E}^T , thus increasing the number of checks on experimental measurements and creating possible new approaches to studies of correlations in multiparticle processes.

We have provided some analytic formulas to assist in the analysis of SBCF data, and have shown that these correlation functions obey the same multiplicity scaling law as scaled factorial moments. Finally, we have shown that SBCF's can be used to selectively study correlations from specific sources. It is possible to (a) split bins in rapidity, (b) split bins in azimuthal angle, (c) construct transverse energy SBCF's, (d) compare results with and without p_T cuts, and (e) use the charge of particles to create tests for various production mechanisms. We

leave it to the readers to investigate further applications of SBCF's, and to test their behavior against different models for high-energy phenomena.

ACKNOWLEDGMENTS

We are grateful to J. Kapusta for helpful comments. S.V. would also like to thank Larry McLerran for hospitality at the Theoretical Physics Institute of the University of Minnesota. D.S. was supported by the U.S. Department of Energy under Contract No. DOE/DE-FG02-87ER-40328. Computer facilities were provided by the Minnesota Supercomputer Institute.

*Electronic address: fvs6325@umnacvx(Bitnet).

†Electronic address: svoloshi@umnacvx(Bitnet); current address: Moscow Engineering Physics Institute, Kashirskoe sh. 31, Moscow 115409, U.S.S.R.

¹S. Voloshin and D. Seibert, Phys. Lett. B **249**, 321 (1990).

²A. Bialas and R. Peschanski, Nucl. Phys. B **273**, 703 (1986).

³D. Seibert, Phys. Rev. D **41**, 3381 (1990).

⁴UA1 Collaboration, B. Bushbeck and P. Lipa, in *Proceedings of the Workshop on Intermittency in High Energy Collisions*,

Santa Fe, NM, 1990, edited by J. Binder (World Scientific, Singapore, 1990).

⁵UA5 Collaboration, G. J. Alner *et al.*, Phys. Rep. **154**, 247 (1987).

⁶A. Bialas and R. Peschanski, Nucl. Phys. B **308**, 857 (1988).

⁷L. Foà, Phys. Rep. **22**, 1 (1975).

⁸K. Fialkowski, B. Wosiek, and J. Wosiek, Acta Phys. Pol. B **20**, 97 (1989).